



日本原子力研究開発機構機関リポジトリ
Japan Atomic Energy Agency Institutional Repository

Title	Estimation of the release time of radio-tellurium during the Fukushima Daiichi Nuclear Power Plant accident and its relationship to individual plant events
Author(s)	Takahashi Sentaro, Kawashima Shigeto, Hidaka Akihide, Tanaka Sota, Takahashi Tomoyuki
Citation	Nuclear Technology,205(5),p.646-654
Text Version	Accepted Manuscript
URL	https://jopss.jaea.go.jp/search/servlet/search?5061182
DOI	https://doi.org/10.1080/00295450.2018.1521186
Right	This is an Accepted Manuscript of an article published by Taylor & Francis in Nuclear Technology on May 2019, available at http://www.tandfonline.com/10.1080/00295450.2018.1521186 .



Estimation of the release time of radio-tellurium during the Fukushima Daiichi Nuclear Power Plant accident and its relationship with individual plant events

Sentaro Takahashi ^{1,2)}, Shigeto Kawashima²⁾, Akihide Hidaka ³⁾, Sota Tanaka²⁾, Tomoyuki Takahashi¹⁾

1) Institute for Integrated Radiation and Nuclear Science, Kyoto University, 2) Graduate School of Agriculture, Kyoto University, 3) Nuclear Human Resource Development Center, Japan Atomic Energy Agency.

Correspondence to: S. Takahashi, Institute for Integrated Radiation and Nuclear Science, Kyoto University, 1-Asashironishi, Kumatori-cho, Sennan, Osaka 590-0494, Japan

sentaro@rri.kyoto-u.ac.jp

pages, 6 figures, and 1 table

Abstract

A simulation model was developed to estimate the areal (surface) deposition pattern of $^{129\text{m}}\text{Te}$ after the Fukushima Daiichi Nuclear Power Plant accident. Using this model, the timing and intensity of the $^{129\text{m}}\text{Te}$ release were reverse estimated from the environmental monitoring data. Validation using ^{137}Cs data showed that the model simulated atmospheric dispersion and estimated surface deposition with relatively high accuracy. The estimated surface deposition pattern of $^{129\text{m}}\text{Te}$ was consistent with the actual measured pattern. The estimated time and activity of $^{129\text{m}}\text{Te}$ emissions indicated that $^{129\text{m}}\text{Te}$ was predominantly emitted from Unit 3.

Key words: Fukushima accident, radio-tellurium, simulation model, deposition pattern, plant events

I. Introduction

A significant amount of radioactive material was discharged into the atmosphere during the Fukushima Daiichi Nuclear Power Plant (FDNPP) accident. The released radioactive material diffused as a radioactive plume and contaminated the environment through wet and dry deposition. Excluding radioactive noble gases, the activity of released radio-tellurium (127m , 129m , ^{131m}Te) was the third largest following radio-iodine and radio-cesium¹⁾. Previously, the authors estimated internal radiation doses due to the uptake of radio-tellurium through ingested food and showed that, in the year following the accident, residents in the region south-southwest of the FDNPP might have been subjected to significant doses of internal radiation from radio-tellurium, which were comparable to the doses due to ingestion of radio-cesium²⁾. Saito et al.³⁾ reported the radioactivity of some radionuclides, including ^{134}Cs , ^{137}Cs , and ^{129m}Te , at many locations in Fukushima Prefecture and its vicinity. According to their report, the regional deposition pattern of ^{129m}Te differed from that of ^{134}Cs and ^{137}Cs . The ratio of $^{129m}\text{Te}/^{137}\text{Cs}$ was significantly higher in the region south-southwest of the plant, suggesting a difference in the source terms and/or the environmental behavior between radio-tellurium and radio-cesium. Several studies of radio-cesium and radio-iodine have been conducted using

the numerical simulation of atmospheric dispersion, reverse estimation of source terms based on environmental monitoring data, and the relationship between the temporal changes in discharge and the plant events⁴⁻¹²). However, little is known about the release of radio-tellurium.

In this study, we estimated the release timings of radio-tellurium using a new approach that employs the least squares method, in which the regional deposition pattern of ^{129m}Te determined by soil measurements was compared with the simulated deposition pattern determined by an advection-diffusion model. We then examined the plant events in each reactor unit that could be responsible for the atmospheric discharge of radio-tellurium.

II. Methodology

Figure 1 shows the location of the simulation area for the meteorological and advection-diffusion models. The area for the meteorological model was centered at latitude 37.488N and longitude 139.937E and divided into 300 x 300 grids in east-west and north-south directions, with an interval of 3 km, and 27 layers in the vertical direction. Meteorological elements (wind direction, wind speed, diffusion coefficient, and precipitation) in the center 100 × 100 grids with 27 vertical layers

were input into the advection-diffusion model. The region utilized for the advection-diffusion model had 100×100 horizontal grids with an interval of 3 km and 27 vertical layers in the central region of the meteorological simulation area. The areas used for the meteorological and advection-diffusion models were designed to agree with those of the previous studies ³⁻⁵).

The parameters used in the simulation were those used commonly for aerosols in radioactive plumes. The same parameters were used for both radio-cesium and radio-tellurium. The dry deposition velocity was set to 0.01 m/s, which is in agreement with the previous studies regarding the diffusion parameter for atmospheric aerosols ^{13, 14}). For wet deposition with precipitation occurring in one grid, we assumed that all radioactive material in the vertical column containing the grid would be affected. The wet deposition rate, $Df(1/h)$, was calculated using the following equation ¹⁵):

$$Df = 1.7 \times 10^{-4} \times R^{0.6} \quad (1)$$

where R (mm/h) is the precipitation intensity.

The meteorological model used in this study was the Advanced Research WRF model (ARW), which is a revised version of the Weather Research and Forecasting model (WRF) for scientific applications. The ARW is a mesoscale meteorological

model developed by the National Center for Atmospheric Research (NCAR) and the National Centers for Environmental Protection (NCEP). The advection-diffusion model developed by Kawashima at the National Institute of Agro-Environmental Sciences was utilized after some improvement^{13, 16)}. This is a Eulerian model, in which three-dimensional grids are set in the region of interest, particles are generated in an arbitrary grid, and advection-diffusion equations are analyzed by different methods. The model is designed so that each calculation process corresponds to a physical phenomenon such as advection, diffusion, emission, and deposition. The three-dimensional advection-diffusion equation used in this study is

$$\frac{\partial M}{\partial t} = -V \cdot \nabla M + \nabla \cdot (K \nabla M) + S_0 - S_i \quad (2)$$

where M is the concentration of the target substance (Bq/m³), V is the wind speed vector (m/s), K is the diffusion coefficient (m²/s), S_0 is the source term (Bq/m³/s), S_i is the sink term (Bq/m³/s), and t is time (s).

The ground surface deposition data of ^{129m}Te were obtained from a report by Saito et al.³⁾. They presented the longitude and latitude of the measurement locations and interpolated the data to fit the grid mesh of the advection-diffusion model.

The initial and boundary conditions were derived from the Grid Point Value

(GPV) data for numerical weather prediction (Mesoscale Spectral Model, MSM) issued by the Japan Meteorological Agency. National Centers for Environmental Prediction Final (NCEP FNL) Operational Global Analysis data were also required for the WRF; e.g., soil water content and soil temperature, which were not available in the GPV (MSM) data. The Global Land Survey (GLS) datasets of the U.S. Geological Survey were used for the numerical maps of topography, elevation, and land utilization. The simulation period was from 01:00 JST March 14, 2011 to 04:00 JST March 18, 2011 (100 h). The period from the start of the accident to March 14 was excluded from the simulation because the wind direction was from the land to the ocean, no precipitation was observed at the FNDPP site, and no significant ground deposition was measured during this period.

The time and intensity of the release (activity of $^{129\text{m}}\text{Te}$ released per unit time) were estimated using the measured land deposition data (soil concentration data by Saito et al.³⁾) and the simulations from the meteorological and advection-diffusion models. To begin the estimation process, the regional deposition of $^{129\text{m}}\text{Te}$ was simulated assuming that $^{129\text{m}}\text{Te}$ was only discharged for one hour of the study period. This simulation was then repeated every hour and the discharged amount was estimated for each hour. To minimize the difference between the actual and

calculated regional deposition patterns, each hourly discharged amount was weighted. The detailed calculation procedures and equations are described below.

1) Data on the meteorological field calculated by the WRF were input into the advection-diffusion model. The release of the reference activity (1.0×10^{15} Bq) was assumed and input into the simulation model for a specific one-hour period of the 100-h simulation period. The deposition pattern was then calculated.

2) The calculation procedure described in 1) was repeated for every hour of the simulation period of T hours and the deposition pattern in the study area (D_n) was determined using equation (3). The estimated deposition pattern (D_E) was calculated using equation (4).

$$D_n = \begin{pmatrix} u_{1\ 1} & \cdots & u_{100\ 1} \\ \vdots & \ddots & \vdots \\ u_{1\ 100} & \cdots & u_{100\ 100} \end{pmatrix} \quad (3)$$

$$D_E = a_1 D_1 + a_2 D_2 + \cdots + a_T D_T \quad (4)$$

Here, u (Bq/m²) refers to the spatial elements in the regional deposition pattern and a is the weighting factor for each hour. Thus, a_n denotes the ratio of the estimated release activity to the reference activity (1.0×10^{15} Bq) at time n . The release activity rate at time E_n (Bq h⁻¹) was calculated as follows.

$$E_n = a_n \times 1.0 \times 10^{15} \quad (5)$$

3) The evaluation function A is the sum of the least squares of the difference between the actual deposition (D_0) and the estimated deposition (D_E), as shown in equation (6). Finally, to minimize the evaluation function A, the weighting factor a_n was determined for each period by nonlinear optimal solution searching.

$$A = \sum_{l=1}^T \sum_{m=1}^T (D_{0 \ l \ m} - D_{E \ l \ m})^2 \quad (6)$$

Here, l and m denote the row and column of the determinant, respectively.

III. Results

III. A. Validation of the simulation model using ^{137}Cs deposition

As described in section II, the simulation parameters were the same for cesium and tellurium. Therefore, the simulation model used in this study was validated with respect to the regional deposition of ^{137}Cs . Temporal changes in the amount of ^{137}Cs released from the FDNPP estimated by Katata et al.¹²⁾ were input into the simulation model. The regional deposition patterns of ^{137}Cs , which were calculated using the simulation model and measured by an airborne survey, are shown in Fig.

2. The estimated deposition characteristics (massive deposition to the northwest of

the FDNPP, relatively high levels of deposition in the central region of Fukushima Prefecture and the northern region of Tochigi Prefecture, and low levels of deposition in the southeastern region of Fukushima Prefecture) were consistent with the measurements. The simulation depicts the deposition of maximum 1×10^5 Bq/m² in the southern region of Miyagi Prefecture (northern from lat. 38.10N), whereas no significant deposition was detected by the airborne survey. In the northern area of Gunma Prefecture, some scattering depositions (more than 1×10^4 Bq/m²) were detected by the airborne survey, but the simulation failed to depict it.

III.B. Estimation of the regional deposition pattern of ^{129m}Te and its relationship with the release events of individual reactor units

Figure 3 shows the estimated regional deposition patterns of ^{129m}Te and the interpolated values of the measured soil concentrations. The simulation model successfully reconstructed the actual deposition patterns. The estimated deposition was within 0.2 - 5.0 times the measured value at 774 out of 1307 grid sections where the ^{129m}Te was detected in soil samples. The exceptions were relatively lower deposition at the southwest region, and a short extension of high-level deposition to the northwest of the FDNPP. The measured deposition at the

southwest region (southern from lat. 37.50N, western from long. 140.40E) was approximately 4.48 times higher in average than the simulated deposition.

The estimated time and amount of the $^{129\text{m}}\text{Te}$ release are shown in Fig. 4. The duration of each release was assumed to be one hour in the simulation; e.g., the release estimated at 01:00 JST indicates the one that occurred between 01:00 and 02:00 JST. Major plant events, including hydrogen explosions, containment vent operations, pressure decreases in the drywell, and visible smoke emissions, are labeled as A–G and summarized in Table 1.

The largest atmospheric release was estimated to occur at 11:00 JST on March 14, coincident with plant event A. Significant releases corresponding to events C, E, F, and G were estimated to occur from 10:00 to 15:00 JST on the same day. No emission of $^{129\text{m}}\text{Te}$ was estimated at the time of events B and D. No major plant events, such as hydrogen explosions or containment vent operations, were reported at 01:00–02:00 JST on March 14, when a significant release was estimated.

IV. Discussion

IV.A. Model suitability

The high level of consistency between the estimated regional deposition pattern of ^{137}Cs and the measurements taken by the airborne survey (Fig. 2) indicates an

accurate simulation by the model used in this study. In the model, 100 x 100 grids with an interval of 3 km were mapped over the entire area of simulation. Thus, a total of 10,000 grid sections were simulated and analyzed. To validate the model for ^{137}Cs , the measured surface deposition was compared with the estimated deposition for 822 grid sections where ^{137}Cs was measured in soil samples. The Pearson product-moment coefficient of the correlation between the estimated and measured depositions was 0.64. This value indicates a relatively high correlation, considering the large deviation between regional deposition patterns, as well as within regions. The validation results for the release and deposition of ^{137}Cs show that the model used in this study can simulate atmospheric dispersion and estimate surface deposition with a relatively high accuracy.

IV. B. Relationship between $^{129\text{m}}\text{Te}$ release behavior and plant events

Some $^{129\text{m}}\text{Te}$ releases corresponded to the occurrence of the major plant events described in Table 1. The earliest release in the simulation period was estimated from 01:00 to 02:00 JST on March 14. Although no major plant events such as hydrogen explosions or containment vent operations were reported at this time, an event could still have occurred leading to the loss of the confinement function of

containment¹⁴⁾. For example, one report¹⁷⁾ indicates that leakages occurred at the upper flange of the containment vessel of Unit 3, although these have not been fully confirmed. Thus, it is possible that this event was responsible for the observed release of radio-tellurium.

A large release of $^{129\text{m}}\text{Te}$ was estimated from 11:00 to 12:00 JST on March 14, which directly corresponded to major plant event A (hydrogen explosion of Unit 3). In many previous reports, the largest release of radionuclides, including ^{137}Cs and ^{131}I , was also estimated at this time. The estimated release of $^{129\text{m}}\text{Te}$ prior to 11:00–12:00 JST on March 14 may also be attributed to Unit 3. It is possible that $^{129\text{m}}\text{Te}$ was released from the reactor building at 10:00–11:00 JST on March 14 after $^{129\text{m}}\text{Te}$ vaporized in the reactor pressure vessel, which experienced damage at 10:40 JST on March 13. Then, $^{129\text{m}}\text{Te}$ leaked to the containment vessel through an open safety valve at 09:05 JST on March 14 and was transferred to the reactor building through the exhaust ventilation of the containment vessel at 09:20 JST on March 14. A relatively large $^{129\text{m}}\text{Te}$ release was also estimated at 12:00–15:00 JST after the Unit 3 hydrogen explosion at 11:00 JST. The accumulated $^{129\text{m}}\text{Te}$ in the Unit 3 reactor building was continuously discharged to the atmosphere due to the damage caused by this hydrogen explosion.

Note that the wind direction was southwesterly and the plume traveled over the Pacific Ocean from 10:00 to 15:00 JST, when a large $^{129\text{m}}\text{Te}$ release was estimated. It is assumed that, after traveling to the ocean (northeast), radio-tellurium in the plume returned to the land after a change in the wind direction at approximately 17:00 JST and was deposited along the coastal area south-southwest of the plant. Figure 5 shows the final deposition pattern of $^{129\text{m}}\text{Te}$ released at 11:00 JST on March 14 and simulated by our model. A significant amount of $^{129\text{m}}\text{Te}$ was deposited on the ground along the coast to the south-southwest of the plant, while high levels of deposition occurred over the ocean. By analyzing the monitoring data from six stations in Ibaragi Prefecture, Terasaka et al.¹⁸⁾ demonstrated that the radioactive plume released at noon on March 14 returned to the southern area of the plant the following day. The radio-tellurium spatial deposition pattern exhibited a distinctive feature from that of radio-caesium. As reported by Saito et al.³⁾, $^{129\text{m}}\text{Te}$ concentrations in the soil were much higher than those of ^{137}Cs in the south-southwest region of the plant and the deposition pattern of $^{129\text{m}}\text{Te}$ was very specific and different from that of radio-caesium. This indicates that this specific $^{129\text{m}}\text{Te}$ deposition pattern was caused by the large release of $^{129\text{m}}\text{Te}$ at 10:00–15:00 JST on March 14.

No release of $^{129\text{m}}\text{Te}$ was estimated at the time of plant event B (containment vent

operation of Unit 2 at 21:30 JST on March 14). Although core damage in Unit 2 began at 19:20 JST on March 14, the containment vessel appeared to remain intact, preventing any release. A small amount of the ^{129m}Te release was estimated to correspond to event C (06:00 JST on March 15). The suppression chamber of Unit 2 was damaged by an explosion at this time; thus, gaseous ^{129m}Te that existed in the containment vessel could have been released to the environment. Another possibility is that hydrogen leaking from Unit 3 exploded in Unit 4 at this time. It is also possible that ^{129m}Te was vaporized in Unit 3, moved to Unit 4 along with hydrogen, and then released to the environment when hydrogen exploded. A small release of ^{129m}Te was estimated during plant events E, F, and G, which were all related to the events of Unit 3. However, no release of ^{129m}Te was estimated at 07:00–11:25 JST on March 15 (plant event D), despite the depressurization of the containment vessel of Unit 2 during which radioactive materials would be expected to be discharged to the environment. Therefore, ^{129m}Te was washed out by the pool-scrubbing effect and a significant portion of ^{129m}Te was transferred into the water in the containment vessel and/or accumulated in water in the basement of the reactor building of Unit 2.

IV.C. Features of source terms during the FDNPP accident

The results show that ^{129m}Te was mainly released from Unit 3 and the

contribution of Unit 2 was not large. Hidaka¹⁹⁾ found that the amounts of ^{131}I and ^{137}Cs in the water that accumulated in the reactor building were larger in Unit 2 than those in Unit 3 owing to different damage locations. Mizokami²⁰⁾ found that the lower portion of the containment vessel (bottom of the suppression pool) was damaged and the upper portion was relatively intact in Unit 2; the upper to middle regions of the containment vessel were damaged in Unit 3 (Fig. 6). These findings indicate that a large portion of $^{129\text{m}}\text{Te}$ was washed out of Unit 2 by the pool-scrubbing effect and not released to the environment. However, $^{129\text{m}}\text{Te}$ may have been transferred to the environment without any interference from the water in Unit 3. Many radioactive nuclides were also released from Unit 1, but the events of Unit 1 were not considered in this study because all released matter was transported away and did not contribute to the contamination of the land.

A previous study on source terms for the FDNPP accident predicted that the released amounts of ^{131}I and ^{137}Cs from Unit 2 were larger than those from Unit 3 because the measured containment depressurization rate indicated that the extent of the containment failure of Unit 2 was larger than that of Unit 3²¹⁾. However, the amounts of ^{131}I and ^{137}Cs released from Unit 3 could be larger than those from Unit 2, similar to the release behavior of $^{129\text{m}}\text{Te}$. The findings can be used to study the

source terms of ^{131}I and ^{137}Cs .

IV.D. Prospects for future research on dose evaluation of radio-tellurium

Unlike radio-cesium and radio-iodine, radio-tellurium has not been extensively studied in relation to the FDNPP accident. Relevant data, such as the discharge mechanism from the reactor, environmental behavior, and radiation dose estimation for humans, are limited. However, as shown in this study, radio-tellurium may be discharged to the environment, where it may pose a significant radiation dose to humans under nuclear power plant accident scenarios. The parameters used in the simulation of the atmospheric transfer and diffusion of radio-tellurium are those commonly used for atmospheric aerosols in radioactive plumes. These parameters are the same those used for cesium. However, these parameters may differ between cesium and tellurium, resulting in errors in the simulation. These points will be further investigated in the future.

The behavior of radio-tellurium in the ecosystems and the radiation exposure of humans has already been analyzed²²⁾, but further research on the source terms and effects of this radionuclide on humans is recommended.

V. Conclusion

The release times of radio-tellurium from the FDNPP accident were estimated using a new approach. The timing and amount of the release were determined with the least squares method using regional $^{129\text{m}}\text{Te}$ deposition patterns from soil measurements and simulated deposition patterns from an advection-diffusion model. The largest amount of $^{129\text{m}}\text{Te}$ releases was estimated to have occurred at 10:00–15:00 JST on March 14, which may be attributed to the hydrogen explosion of Unit 3. The release time corresponded to an event at plant 3 but not to events at plants 1 and 2. The approach developed in this study can be used estimate the temporal changes in the amount of released $^{129\text{m}}\text{Te}$ using the final deposition pattern.

VI. Acknowledgements

This work was supported by the Research on the Health Effects of Radiation organized by the Ministry of the Environment, Japan.

VII. References

- [1] UNSCEAR., “Levels and effects of radiation exposure due to the nuclear accident after the 2011 great east-Japan earthquake and tsunami,” UNSCEAR 2013 Report. Annex A, (2014).
- [2] K. Fujiwara, T. Takahashi and S. Takahashi, “Committed Effective Dose from the Oral Ingestion of Radio-tellurium in Rice Released by the Fukushima Nuclear Power Plant Accident,” *Jpn. J. Health Phys.*, **51**,1,19 (2016).
- [3] K. Saito et al., “Detail deposition density maps constructed by large-scale soil sampling for gamma-ray emitting radioactive nuclides from the Fukushima Dai-ichi Nuclear Power Plant accident,” *J Environ Radioact.*, **139**,308 (2015).
- [4] M. Chino et al., “Preliminary estimation of release amounts of I-131 and Cs-137 accidentally discharged from the Fukushima Daiichi Nuclear Power Plant into the atmosphere,” *J. Nucl. Sci. Technol.*, **48**,7, 481129 (2011).
- [5] Y. Morino, T. Ohara and M. Nishizawa., “Atmospheric behavior. deposition. and budget of radioactive materials from the Fukushima Daiichi nuclear power plant in March 2011,” *Geophysical Re. Letters.*, **38**, L00G11(2011).
- [6] T. Yasunari et al., “Cesium-137 deposition and contamination of Japanese soils due to the Fukushima nuclear accident,” *Proc. National Acad. Sci.*, **108**,49,19530 (2011).
- [7] G. Katata et al., “Numerical reconstruction of high dose rate zones due to the Fukushima

- Dai-ichi Nuclear Power Plant accident,” *J Environ Radioact.*, **111**,2 (2012).
- [8] H. Terada et al.,“Atmospheric discharge and dispersion of radionuclides during the Fukushima Dai-ichi Nuclear Power Plant accident. Part II: verification of the source term and analysis of regional-scale atmospheric dispersion,” *J Environ Radioact.*,**112**,141 (2012).
- [9] G. Katata et al.,“Atmospheric discharge and dispersion of radionuclides during the Fukushima Dai-ichi Nuclear Power Plant accident. Part I: Source term estimation and local-scale atmospheric dispersion in early phase of the accident,” *J Environ Radioact.*,**109**,103 (2014).
- [10] C. V. Srinvas et al.,“Regional scale atmospheric dispersion simulation of accidental releases of radionuclides from Fukushima Dai-ichi reactor,” *Atmos. Environ.*, **61**, 66 (2012).
- [11] I. Korsakissok, A. Mathieu and D. Didier,” Atmospheric dispersion and ground deposition induced by the Fukushima Nuclear Power Plant accident: A local-scale simulation and sensitivity study,” *Atmos. Environ.*, **70**, 267 (2013).
- [12] G. Katata et al.,“Detailed source term estimation of the atmospheric release for the Fukushima Daiichi Nuclear Power Station accident by coupling simulations of an atmospheric dispersion model with an improved deposition scheme and oceanic dispersion model,” *Atmos. Chem. Phys.*, **15**,1029 (2014).

- [13] S. Kawashima and S. Takahashi, "An improved simulation of mesoscale dispersion of airborne cedar pollen using a flowering-time map," *Grana.*, **38**,316 (1999).
- [14] "Final report of the investigation and inspection committee on the accident at Fukushima Nuclear Power Stations of Tokyo Electric Power Company," *Tokyo Electric Power Company*, November 26, 2015. Available from; <http://www.cas.go.jp/jp/seisaku/icanps/post-2.html>. Japanese.
- [15] A. Baklanov, and J.H. Sørensen., "Parameterisation of radionuclide deposition in atmospheric long-range transport modelling," *Phys.Chem.Earth, Part B: Hydrology, Oceans and Atmosphere*, **26**, 787-799 (2001).
- [16] S. Kawashima and Y. Takahashi., "Modeling and simulation of mesoscale dispersion processes for airborne cedar pollen," *Grana.*, **34**,142 (1995).
- [17] "Results of χ ray spectrum measurement at the operation floor of reactor building at Unit 2," *Tokyo Electric Power Company*, November 26, 2015. Available from; http://www.meti.go.jp/earthquake/nuclear/decommissioning/committee/osensuitaisakuteam/2015/pdf/1126_3_2f.pdf. Japanese.
- [18] Y. Terasaka, et al., "Air concentration estimation of radionuclides discharged from Fukushima Daiichi nuclear power station using NaI(Tl) detector pulse height distribution

- measured in Ibaraki Prefecture. *J. Nucl. Sci. Tech.*, 53: 1919-1932, (2016).
- [19] A. Hidaka and J. Ishikawa., “Quantities of I-131 and Cs-137 in accumulated water in the basements of reactor buildings in process of core cooling at Fukushima Daiichi nuclear power plants accident and its influence on late phase source terms,” *J. Nucl. Sci. Technol.*, **51,4**, 413 (2014).
- [20] S. Mizokami., “Progress of evaluation of RPV/PCV-status of FDNPS,” *CLADS workshop as Fukushima Research Conference for “Dialog on Fuel/Core Degradation in Severe Accident among Experts of Material Science, Thermodynamics, Severe Accident Analysis and Modeling”* (2017), Iwaki, Japan. July 5, Japan Atomic Energy Agency(2017).
- [21] H. Hoshi et al., “Computational analysis on accident progression of Fukushima Daiichi NPS.” *In: Proc. PSAM2013-1061 Tokyo. Probabilistic Safety Assessment and Management (2013)*, Tokyo, Japan. April 13-18, Atomic Energy Society of Japan(2013).
- [22] K. Fujiwara et al., “Transfer factors of tellurium and cesium from soil to radish (*Raphanus sativus* var. *sativus*) and Komatsuna (*Brassica rapa* var. *perviridis*),” *Jpn. J. Health Physics.*, in press (2018).

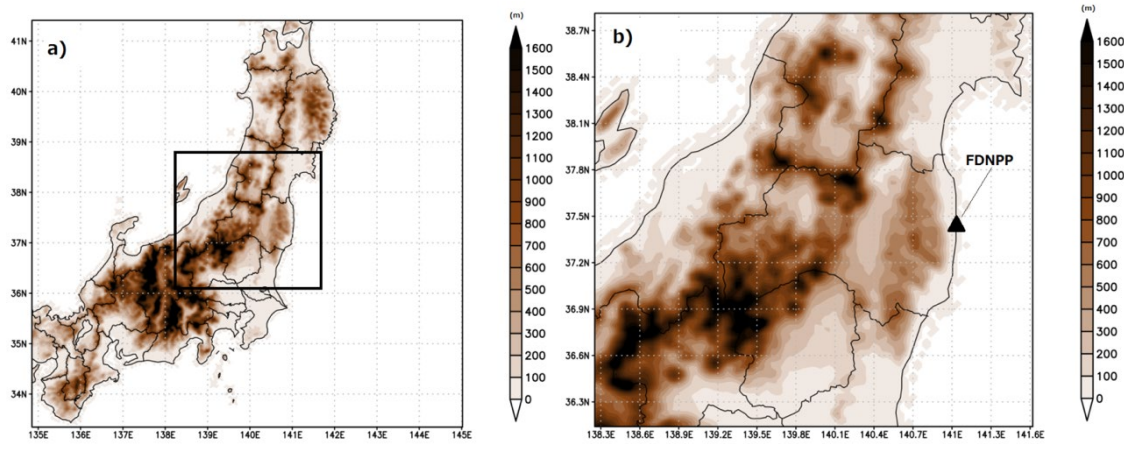


Fig. 1 Location of the simulation area for a) the meteorological model and b) the advection-diffusion model.

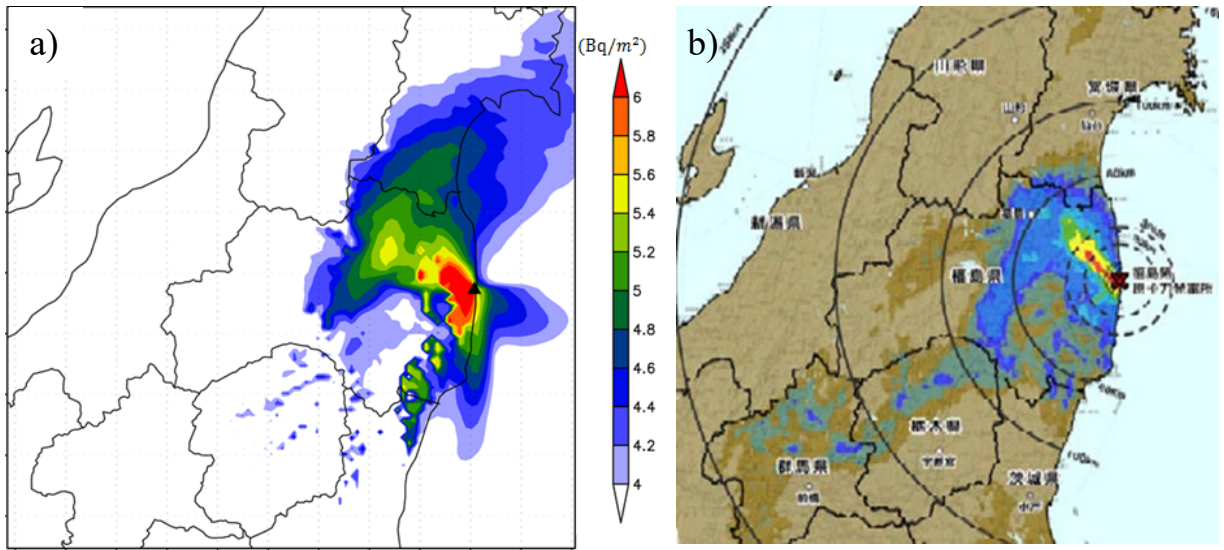


Fig. 2 Regional deposition patterns of ^{137}Cs simulated in this study a) and measured in the airborne survey b).

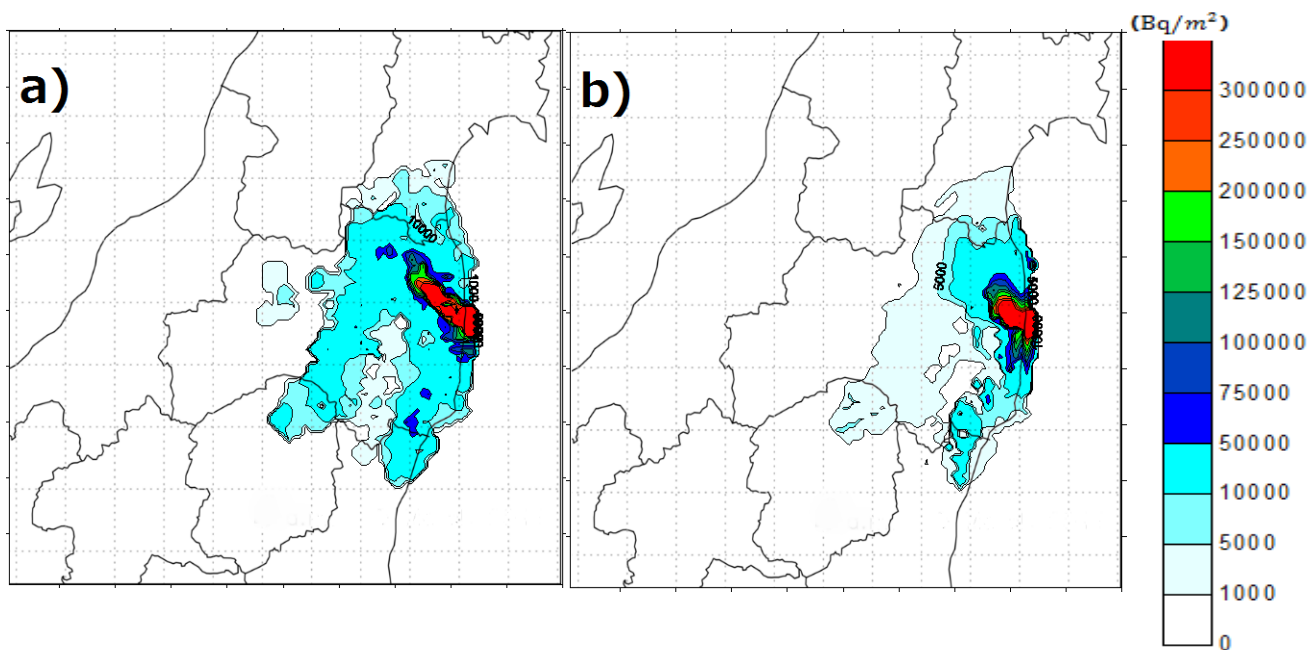


Fig. 3 Measured soil concentrations a) and estimated deposition patterns b) of ^{129m}Te .

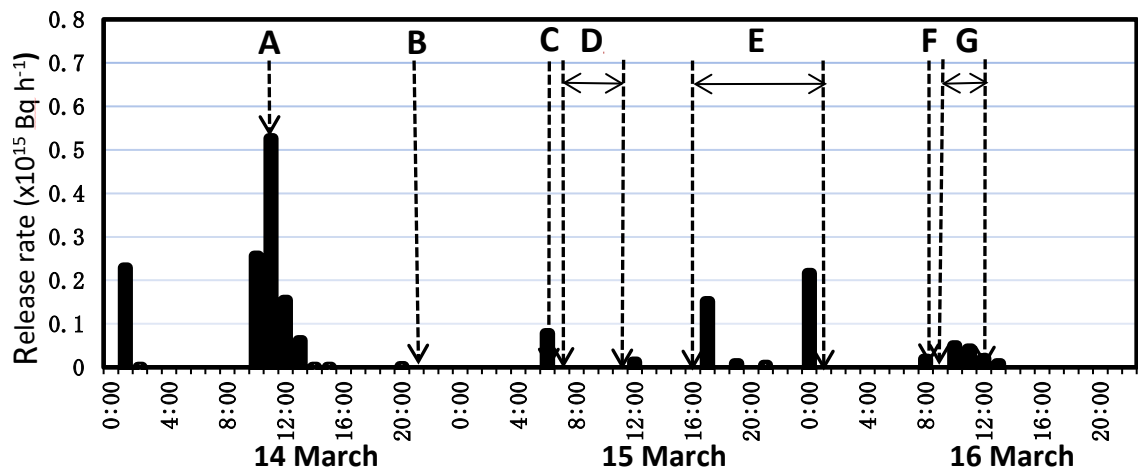


Fig. 4 Estimated time and amount of ^{129m}Te release and major plant events.

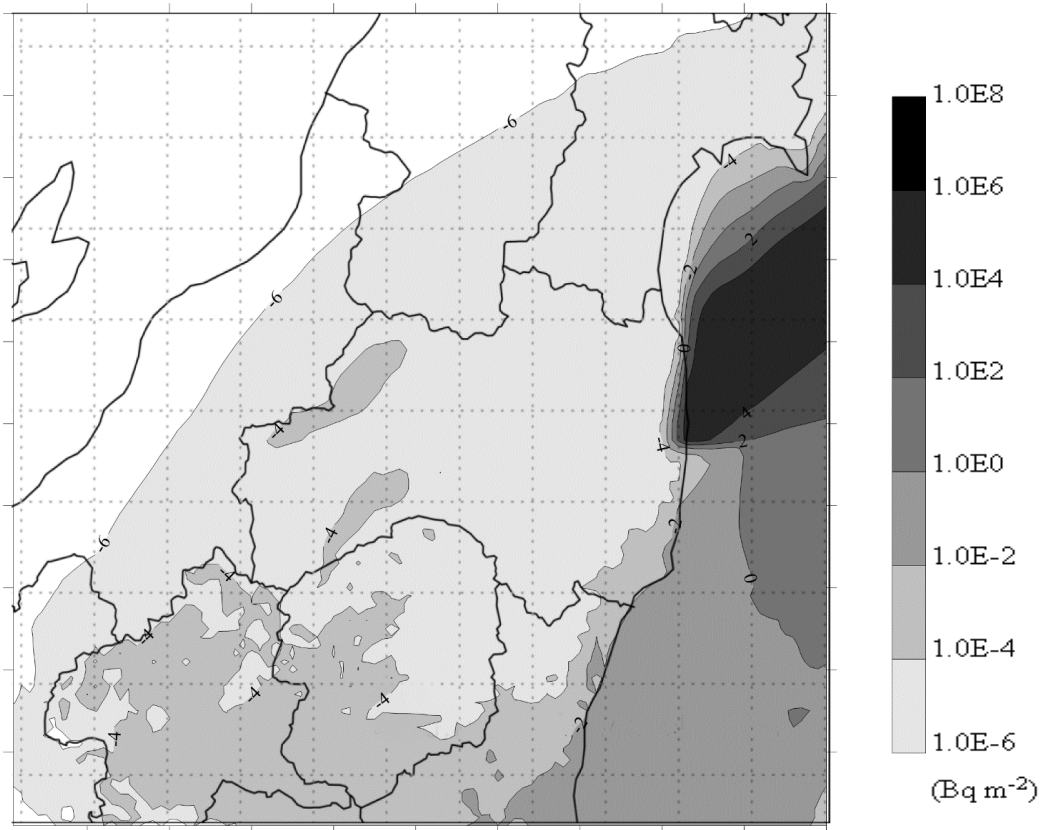


Fig. 5 Final deposition pattern of ^{129m}Te released at 11:00–12:00 JST on March 14. The majority of ^{129m}Te was deposited over the ocean, but some was deposited on land and formed the specific deposition pattern of ^{129m}Te to the south-southwest of the plant.

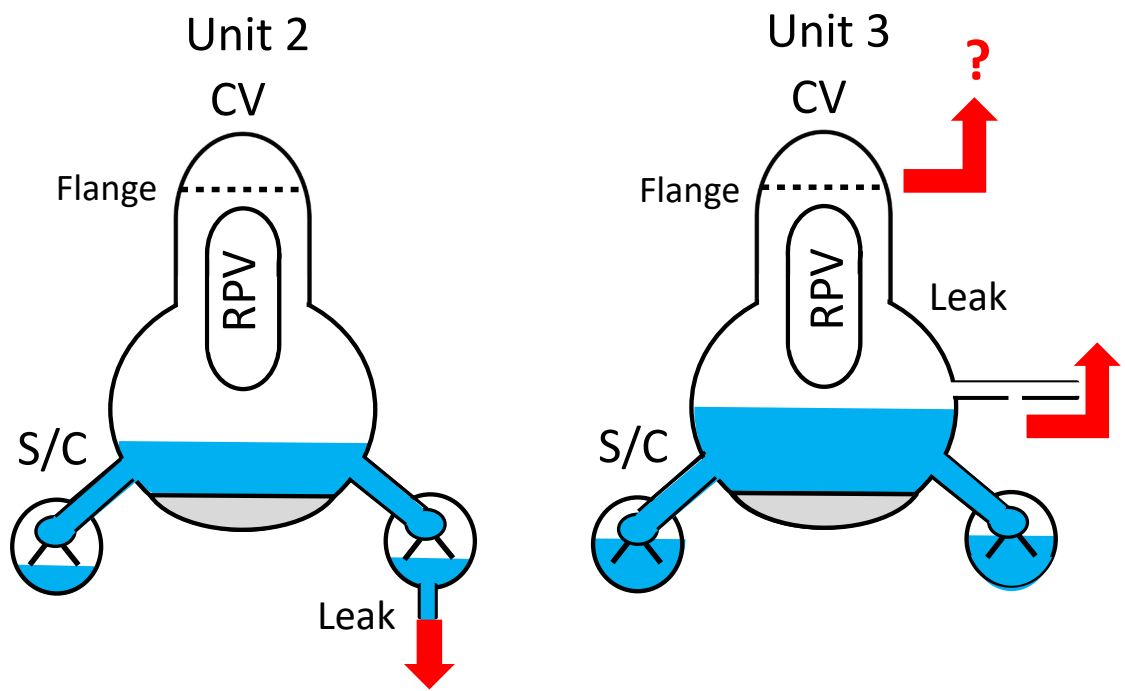


Fig. 6 Images showing the difference in CV failure location between Units 2 and 3

Table 1 Details of major plant events shown in Fig. 4

Labels in Fig. 4	Time of occurrence	Events
A	3/14 11:01	Unit 3, hydrogen explosion and collapse of building
B	3/14 21:30	Unit 2, containment vent operation and atmospheric discharge
C	3/15 Approx. 6:00	Unit 2, sound of explosion (probably steam explosion). Unit 4, hydrogen explosion.
D	3/15 7:00–11:25	Unit 2, pressure decrease in drywell
E	3/15 16:00–3/16 1:00	Unit 3, containment vent operation. Unit 2 & 3, pressure decrease in drywell
F	3/16 Approx. 8:30	Unit 3, white smoke emission
G	3/16 9:00–12:00	Unit 3, pressure decrease in drywell